

ISM Cheat Sheet

January 6, 2020

1 Concepts

1.1 Introduction: Ecology of the Interstellar Medium

1.1.1 What does the ISM consist of?

Most of the "empty" space in the universe is filled by the ISM. The ISM consists of

1. hydrogen, helium, traces of metals
2. ionized, neutral and molecular constituents
3. gas phase and solid states
4. magnetic fields
5. cosmic rays (relativistic particles)

Far most of the ISM consists of hydrogen and helium.

1.1.2 Phases of the ISM and their global properties

In the ISM we consider different phases at different temperatures, densities and filling factors.

1. Hot ionized medium: temperature about 1 million degrees, densities of approximately $4 \cdot 10^{-3} \text{ cm}^{-3}$ and a filling factor of over 50%.
2. Warm ionized medium: temperature about 8000 K, densities of approximately $2 \cdot 10^{-1} \text{ cm}^{-3}$ and a filling factor of 10%.
3. Warm neutral medium: 5000 K, $6 \cdot 10^{-1} \text{ cm}^{-3}$ and about 40% filling factor.
4. Cold neutral medium, which is about 100 K, has high densities of $3 \cdot 10^1 \text{ cm}^{-3}$ and a low filling factor of approximately 1%. The warm neutral medium does not have a continuous distribution. The cold neutral medium is found mainly in clouds.

Furthermore we still have molecular clouds and HII regions which could be considered as ISM phases, however their filling factors are extremely small and hence for the large overview they are not important.

1.1.3 What are the sources of energy in the ISM?

The main sources of energy in the ISM are: radiation, magnetic fields, cosmic rays and mechanical energy. All energy densities are of comparable magnitude and about 0.5 eV cm^{-3} . The 3K cosmic background radiation is not coupled to anything else. The thermal, hydrodynamical and magnetic energy are coupled magnetohydrodynamically. Thermal energy and starlight are naturally weakly coupled. The ISM is not in thermodynamic equilibrium. This makes sense as there is no process that can counterbalance the energy added into the ISM by stars.

1.2 Review of radiative processes

1.2.1 Excitation temperature

The excitation temperature is defined per transition, and such that

$$\frac{n_u}{n_l} = \frac{g_u}{g_l} e^{-(E_u - E_l)/kT_{ex}}$$

In general, the excitation temperature T_{ex} is not equal to the kinetic energy T_{kin} . If this is the case, level populations are called thermalized. If the excitation temperature is below the kinetic energy, we speak of subthermal excitation.

1.2.2 Equilibrium

The Maxwell distribution is valid in the ISM. Elastic collisions are sufficiently frequent to thermalize velocity distributions.

The Planck distribution is generally not valid in the ISM, as the interstellar radiation field deviates strongly from a Planck function.

The Boltzmann distribution is not generally valid in the ISM. We use it to define an excitation temperature as above. Statistical equilibrium is a weaker condition than thermodynamic equilibrium (=detailed balance). Statistical equilibrium dictates that the sum of rates of processes populating level i equals the sum of rates of all processes depopulating level i .

1.3 Interaction of radiation with matter

1.3.1 When is stimulated emission (un)important?

1.4 Radiative transfer

$$T_B = T_{background} e^{-\tau_0} + T_{source}(1 - e^{-\tau_0})$$
$$I_B = \frac{2k}{\lambda^2} [T_{background} e^{-\tau_0} + T_{source}(1 - e^{-\tau_0})]$$

1.4.1 Pure absorption line

1.4.2 Masers

Maser emission can occur when the process of populating a certain energy level is easier than that of other, lower levels. To have a maser in the $i \rightarrow j$ transition we need that

$$\frac{n_i}{n_j} > \frac{g_i}{g_j}$$

Maser lines are very bright, narrow and peaked. Some known molecules with maser transitions are OH, H₂O, NH₃, H₂CO, CH₃OH, HCN, etc. To have maser emission, we need a strong IR radiation field and very high densities.

1.5 The Atomic Medium

1.5.1 The H1 21cm line and the concept of spin temperature

The 21cm line is caused by a hyperfine structure transition in the ground electronic state of H1 (coupling of electron and nuclear spins). Thus electron spins parallel to antiparallel cause this transition. The spin temperature is the excitation temperature of H1.

1.5.2 Combining HI emission and absorption observations to derive optical depth

In cases where we have a bright background radio source with a continuum spectrum (a typical radio-loud quasar or an active galactic nucleus or a radio galaxy), we can study both emission and absorption by the foreground interstellar medium in our galaxy by comparing "on source" and "off source" observations. The technique consists of taking on-source observations with the radio telescope pointed at the background radio source, and off-source observations with the telescope pointed so that the background source is out of the beam (and we are observing black sky behind the foreground cloud). We assume the foreground gas is sufficiently uniform so that the two different signal lines have essentially the same $N(HI)$ and T_{spin} .

We measure the on source and off source spectra T_A^{on} and T_A^{off} , where we continue to report frequency (shifts) in terms of radial velocity. From the measurements at frequencies well above and below the 21-cm line emission feature, we determine the antenna temperature T_{sky} of the blank sky, and the antenna temperature T_{RS} of the continuum from the radio source. At velocity V , the spectrum measured on the blank sky is

$$T_A^{off}(v) = T_{sky} e^{-\tau_v} + T_{spin}(1 - e^{-\tau_v})$$

While the spectrum on the radio source is

$$T_A^{on}(\nu) = T_{RS}e^{-\tau_\nu} + T_{spin}(1 - e^{-\tau_\nu})$$

These two equations can be solved for the unknown $\tau(\nu)$ and $T_{spin}(\nu)$.

$$\tau(\nu) = \ln \left[\frac{T_{RS} - T_{sky}}{T_A^{on}(\nu) - T_A^{off}(\nu)} \right]$$

$$T_{spin}(\nu) = \frac{T_A^{off}(\nu)T_{RS} - T_A^{on}(\nu)T_{sky}}{(T_{RS} - T_{sky}) - [T_A^{on}(\nu) - T_A^{off}(\nu)]}$$

1.5.3 When is HI observed in emission and when in absorption?

We observe HI in absorption if there is a cloud of gas between a radio source and the observer that does not outshine the cold gas. Eg if we have a moderately cold cloud of gas between the radio source and observer, we will detect HI in absorption. If we look at a warm gas cloud however, we will observe the gas and thus detect HI in emission. This is evidence for the two-phase ISM.

1.5.4 2-phase neutral ISM (CNM, WNM)

The evidence is, as described above, that we detect HI in both absorption (CNM) and emission (WNM). A cold cloud has a high optical depth, and temperatures below 100 K. A warm cloud has temperatures of about 5000 K and a low optical depth. The optical depth scales linear with the column density and inversely with the (spin) temperature.

1.5.5 Absorption lines to determine abundances

?

1.6 Ionization and Recombination

1.6.1 Photoionization of atomic hydrogen and the approximate shape of the photoionization cross section

The ionization edge is at 13.6 eV, or 912 Å. Recombination lines result from the downward cascade following recombination in ionized gas. Recombination to the ground-state leads to ionizing photons which lead to ionization immediately (on the spot approximation). Recombination spectrum is independent of density. The temperature comes in through the T-dependence of recombination coefficient α but the temperature of HII regions is fairly uniform 5000-10000 K, so there is only a weak temperature dependence. Radio recombination lines are much more complicated since we need to deal with density dependence and stimulated emission.

The recombination process of hydrogen is independent of density.

1.6.2 Case A and case B recombination

Case A recombination is the process where photons above 13.6 eV are re-absorbed. In case B recombination, these photons are not re-absorbed. The two cases have different recombination coefficients.

1.6.3 Ratios

Ratios for the different lines are quite fixed, although there is a small temperature dependence. We can use these theoretical ratios to derive extinction. The problem on the problem set on this should be known.

1.7 HII regions

1.7.1 Strömgren sphere

Strömgren spheres are ionization bounded. This means that the nebula absorbs all ionizing photons from the star. There is thus no more gas that can be ionized. Some HII regions are density bounded (for example planetary nebulae). This means that UV photons escape the nebula. Some photons are also absorbed by dust. This will suppress emission lines, radio continuum, radius etc. Strömgren spheres can be calculated by considering how many hydrogen atoms can be ionized by UV photons from the star. For the Strömgren sphere, we have that

$$Q_0 = \frac{4\pi R_{S0}^3 \alpha_B n(H^+) n_e}{3}$$

And, since $n(H^+) = n_e = n_H$, we can solve for the Strömgren sphere.

$$R_{S0} = \left(\frac{3Q_0}{4\pi n_H^2 \alpha_B} \right)^{1/3}$$

If densities become higher, the Strömgren spheres become smaller. Therefore the fraction of ionization goes up and thus dust becomes more important in absorbing photons.

1.7.2 Emission measure

The emission measure (EM) is defined by

$$EM = \int n_e n_p ds = \left[\frac{n_e n_p}{k_{ff,v}} \right]_T \tau_v$$

For small optical depth, I_ν increases linearly with the emission measure. The emission (in UV, optical, IR recombination lines and radio continuum) from an HII region is proportional to the emission measure and therefore to the square of the density.

1.7.3 Star formation rate

The recombination line luminosity is a measure for the star formation rate. Young massive stars produce copious amounts of ionising photons that ionise the surrounding gas. Only stars more massive than $M \sim 20 M_\odot$ produce a measurable amount of ionising photon flux. Mostly, SFR regions are ionisation bound (eg all UV is absorbed and does not leak out of the system). Due to inhomogeneities in the ISM, some fraction of the ionising photons might leak out however. We make assumptions for the stellar masses, temperatures, electron densities and ages. Furthermore we need to assume:

1. Constant SFR
2. Scaling IMF, massive stars are rare, low mass stars are common. Thus we need to scale
3. Need to assume a star formation history

1.7.4 HII region evolution

HII regions gradually expand due to the thermal pressure. Very young HII regions, born in very dense molecular clouds are very small and dense. Due to the expansion, a dense layer builds up at the ionization front.

1.7.5 Boundaries

1. Ionization bounded: nebula absorbs all ionizing photons from the star. There is more gas that could be ionized, but there are no more photons
2. Density bounded: UV photons escape the nebula, there are thus remaining photons when we are out of gas
3. Dust bounded: UV photons are absorbed by the dust. This suppresses emission lines, radio continuum, etc. dust may even be dominant in dust-bounded HII regions.

1.8 Collisional excitation

1.8.1 2 level system

In a two level system we have the following processes: absorption, spontaneous emission, stimulated emission, collisional excitation, collisional de-excitation. Collisional (de-)excitation scales with the density of the collision partner and the density of the species itself. We can scale upward and downward collision rates using

$$k_{01} = k_{10} e^{-E_{10}/k_B T} \frac{g_1}{g_0}$$

We can write down the differential equation for the number of the species in a given level. Below is this without absorption and stimulated emission.

$$\frac{dn_1}{dt} = -n_1 A_{10} + n_0 n_c k_{01} - n_1 n_c k_{10}$$

1.8.2 Critical density

For a collision partner c , we define the critical density $n_{crit,u}(c)$ for an excited state u to be the density for which collisional deexcitation equals radiative deexcitation, including stimulated emission.

$$n_{crit} = \frac{A_{10}}{k_{10}}$$

There are two limiting cases:

1. $n_c \gg n_{crit}$:

$$\frac{n_1}{n_2} = \frac{g_1}{g_2} e^{-E_{10}/kT}$$

For this situation, the levels are thermalized, we have that $T_{ex} = T_{kin}$ and level populations are independent of n_c .

2. $n_c \ll n_{crit}$:

$$\frac{n_1}{n_0} = \frac{n_c}{n_{crit}} \frac{g_1}{g_0} e^{-E_{10}/kT}$$

For this situation, $T_{ex} < T_{kin}$, subthermal excitation and level populations depend on the density of the collision partner.

We can use this to determine if a given species is a temperature or density probe.

1.8.3 Adding radiation

We define a direction averages radiation field:

$$\bar{n}_\gamma = \frac{c^2}{8\pi h \nu^3} u_\nu$$

And the photon occupation number

$$u_\gamma = \frac{1}{\exp(h\nu/kT_r) - 1}$$

Now we get for the complete (5 fold) differential equation

$$\frac{dn_1}{dt} = n_0 n_c k_{01} - n_1 n_c k_{10} + \left[n_0 \bar{n}_\gamma \frac{g_1}{g_0} - n_1 (1 + \bar{n}_\gamma) \right] A_{10}$$

Where $n_0 \bar{n}_\gamma \frac{g_1}{g_0} A_{10}$ is the absorption and $-[n_1 (1 + \bar{n}_\gamma)] A_{10}$ the spontaneous plus stimulated emission. We need this complete result in molecular clouds and when lines are optically thick because of absorption. This gives a steady state

$$\frac{n_1}{n_0} = \frac{n_c k_{01} + \bar{n}_\gamma \frac{g_1}{g_0} A_{10}}{n_c k_{10} + (1 + \bar{n}_\gamma) A_{10}}$$

We can use this to define the critical density in a more general way

$$n_{crit} = \frac{(1 + \bar{n}_\gamma) A_{10}}{k_{10}}$$

1.8.4 HI 21cm line

For the 21 cm line we have

$$\frac{E_{10}}{k} = 0.0682 \text{ K}$$

$$A_0 = 2.88 \cdot 10^{-15} \text{ s}^{-1}$$

$$k_{10} = 1.2 \cdot 10^{-10} \text{ cm}^{-3} \text{ s}^{-1}$$

We find a radiation temperature of

$$T_r = 2.73 \text{ K} + 1 \text{ K} = 3.73 \text{ K}$$

1.8.5 Nebular diagnostics

A line is a temperature diagnostic if the line has different upper levels, bracketing T_{kin} and the line is a density diagnostic if it has similar upper levels but different critical densities.

SII: At low densities, every collisional excitation of both of the SII levels will be followed by a radiative decay. Therefore, in the low density limit, the power radiated in both of the lines is simply proportional to the collision rates. At higher densities, the levels become thermalized. Now the ratio of radiated power in the two levels will no longer be set by the ratio of collision rates. This gives the transition from 1.4 to 0.5.

1.9 Molecules and molecular excitation

1.9.1 Energy levels of simple molecules and their transitions

The rotational levels of simple (linear) molecules are described by

$$E_{rot} = \frac{\hbar^2}{2r_n^2 m_r} J(J+1)$$

This scales roughly with J^2 .

1.9.2 Why we cannot use H₂ to measure molecular gas masses

The first allowed and observable H₂ transition has an excitation temperature (500K) well above the average temperature of a molecular cloud (20K). H₂ lines are only observable from space and thus expensive. The last reason not to use H₂ is that the first transition is a quadrupole and the line is thus faint.

1.9.3 Why CO is a good tracer

Since CO has a lower excitation temperature (5.5K) than H₂, this is easily excited and thus observable in the average molecular cloud. CO also has the right critical density and its abundance is relatively high (although orders below that of H₂). CO is thus a good tracer for the conditions in the ISM.

1.9.4 Other molecules

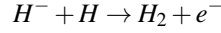
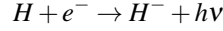
Most other simple molecules, like HCN, HCO⁺, CN, etc trace higher densities than CO.

1.9.5 Higher rotational levels probe higher temperatures and higher densities

As shown before, the rotational energy scales roughly with J^2 . Higher J thus have higher energies. This naturally leads to higher J levels tracing higher temperature regions and higher density regions (since there, these levels are more easily excited).

1.9.6 How is H₂ formed?

H₂ is formed in two ways. Either in two steps where an electron is used as catalyst:



This is how the first H₂ molecule in the universe is produced. However, the rate of this formation is too low to reproduce the abundances we find. A second, more efficient, way of H₂ formation is on the surface of dust grains.

1.9.7 Photodissociation of H₂ and self-shielding

Due to self-shielding, lines become optically thick very fast. Thus the value we find for the dissociation rate is the dissociation rate at the surface of the cloud, not at the inner regions. Self shielding increases the efficiency of H₂ formation inside molecular clouds.

1.10 Thermal balance

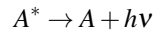
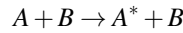
1.10.1 Equation of thermal balance, including heating and cooling rates

In the ISM, we have the following heating mechanisms:

1. Radiative heating: starlight and radiation from an AGN
2. Mechanical heating: shock waves and dissipation of turbulence
3. Cosmic ray heating

We have the following cooling mechanisms:

1. Gas cooling: collisions are crucially important because they provide the cooling of the ISM. Cooling normally proceeds by collisional excitation followed by the emission of a photon, where the photon can escape



To find the temperature, we need to have

$$\Sigma \Gamma(T) = \Sigma \Lambda(T)$$

Usually, $\Lambda(T)$ does not depend on the temperature. HII regions always have a temperature of about 8000-10000 K. Cosmic ray heating penetrates very deep, whereas starlight does not reach very far in the ISM. In some cases, cosmic ray heating can become the dominant heating mechanism in a cloud.

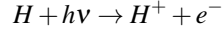
1.10.2 Efficient cooling

To have efficient cooling in the ISM, we need the following things:

1. Frequent collisions
2. Excitation energy comparable to or less than thermal kinetic energy
3. High probability of excitation during collision
4. Photon emission before the next collision
5. No re-absorption of the photon (low optical depth of gas to the line emission)

1.10.3 Heating of HII regions by UV photons

For an HII region, the candidate heating source will be a central star. In general, this is the only source of ionization.



Where $E = 13.6\text{ eV}$ goes into the kinetic energy of the electron. The heating rate is given by

$$\Gamma_{pi}(H) = \alpha_B n_e n_H \psi k T_C$$

Where T_C is the color temperature of the star.

1.10.4 Cooling of HII regions by collisionally excited lines

The cooling rate from collisional excitation is given by Λ_{CE} . If we consider only cooling with recombination lines and free free emission we get the following heat balance.

$$\alpha_B n_H n_e \psi k T_C = \alpha_B n_H n_e (1.22 k T_e)$$

Which yields

$$T_e = \frac{\psi}{1.22} T_C$$

Clearly, this is now enough, since the temperature of an HII region is around 10,000K, whereas the color temperature of an OB star is $> 30,000\text{ K}$. We thus need another way to cool the gas. Dust emission cannot help cooling because the dust and gas are not thermally coupled. Thus, in order to cool the gas, we need to radiate away photons. This is done by photons originating in a transition. Collisionally excited lines will cool the gas both in HII regions, molecular clouds, etc. Important cooling lines are:

1. [OIII]
2. [OII]
3. [SII]
4. [SIII]
5. [NII]

1.10.5 Resulting temperature of HII regions and why they are always about the same temperature

1.10.6 Existence of stable 2-phase neutral ISM (CNM and WNM)

The pressure of the ISM is set by

1. Hydrostatic equilibrium because of gravitational potential
2. Thermal pressure
3. We can measure the pressure independent of theory

If one fixes the pressure and equates where heating and cooling balance, we find two regions. One at high temperature (6000K) and one at low temperature (100K). These two regions are respectively the WNM and CNM. There is no region in between these because such a situation is unstable. If the temperature is perturbed into a temperature in between (thus CNM up or WNM down), thermal balance will return to one of the two situations.

1.10.7 Heating of molecular clouds

Because of optical depth, only the outer regions of a molecular cloud can be reached by starlight / radiation. At the edges of a molecular cloud, we thus have primarily stellar heating. In the interiors however, stellar light cannot penetrate. Here we will thus have primarily CR heating, since CRs penetrate deeper into a cloud.

1.10.8 Cooling of molecular clouds

Molecular clouds have two main cooling mechanisms:

1. In the interior of the cloud, we mainly have molecular rotational lines.
2. At the edges of the cloud, we have fine structure lines.

1.11 Interstellar dust

1.11.1 Extinction for the two limiting cases $\lambda \ll a$ and $\lambda \gg a$

If $\lambda \ll a$, the dust grain is basically a big obscuring screen. We are in the limit of geometric optics. Here, the dependence on λ is weak. The other case, where $\lambda \gg a$, we have Rayleigh scattering. This is the same process that makes the sky look blue. For this regime we have

$$\tau(\lambda) = \int \kappa_D(\lambda) dl$$

Where κ_D is the dust absorption coefficient. Extinction cross sections scale as

$$C_{abs} \propto \frac{1}{\lambda^2} \quad C_{scat} \propto \frac{1}{\lambda^4}$$

1.11.2 Extinction curve

The most important feature of the extinction curve is that it decreases with wavelength (or increases with wavenumber). There is an aromatic feature at 2175\AA and some silicates at $\lambda = 10\text{ }\mu\text{m}$ and C-H bonds at $\lambda = 3.4\text{ }\mu\text{m}$.

1.11.3 Extinction and reddening

The relation between extinction (A_V) and reddening ($E(B_V)$) is given by

$$R_V = \frac{A_V}{A_B - A_V} = \frac{A_V}{E(B_V)}$$

Sightlines through the diffuse gas in the Milky Way have $R_V \approx 3.1$ as an average value.

1.11.4 Composition of dust grains

From UV extinction, scattering of visible light and polarization of starlight, it is clear that the interstellar grain population must have a broad size distribution, extending from sizes as small as $a \approx 0.01\text{ }\mu\text{m}$ to sizes of $a \approx 0.2\text{ }\mu\text{m}$. In fact, we will see that observations of infrared emission require that the size distribution extend down to grains containing as few as ~ 50 atoms, corresponding to sizes of $a \approx 3.5\text{ \AA} = 3.5 \cdot 10^{-4}\text{ }\mu\text{m}$ and also that the largest dust grains extend to sizes of over $100\text{ }\mu\text{m}$.

Dust is composed of heavy elements ($M_{>He} \approx 1\%M_H$). By mass, most of the heavy elements are embedded in dust. Indeed, $\frac{M_{grain}}{M_H} \approx 0.01$. We have a power law of distribution of grain sizes with $a_{min} = 0.005\text{ }\mu\text{m}$ and $a_{max} = 0.25\text{ mm}$.

$$\frac{dn_{grain}}{da} = An_H a^{-3.5}$$

Very prominent features are PAHS, polycyclic aromatics. Little plates of graphite, which form the border between molecules and dust grains. They have no real emission lines, rather bands related to vibrational modes.

1.11.5 Thermal balance of dust grains

Radiative heating: When an optical or UV photon is absorbed by a grain, an electron is raised into an excited electronic state. If the electron is sufficiently energetic, it may be able to escape from the solid as a "photoelectron". In rare cases, the grain will "luminesce": excited state will decay radiatively.

Collisional heating: Collisional heating can be ignored in the CNM, but it can be important within dark clouds (since we have high gas density and very low penetration of UV and optical photons).

Radiative cooling: Grains lose energy by infrared emission. We get a balance between heating and cooling and depending on the intensity of the starlight, we will get either a fluctuation temperature, or a constant balanced temperature for the dust grains.

1.11.6 Emission by dust grains

Emission of dust grains is in the infrared. See above for more.

1.11.7 Modified black body

1.11.8 Thermal spiking of very small dust grains

If the vibrational energy at the steady state temperature of a dust grain is lower than the mean photon energy of an absorbed (heating) photon, the dust temperature will have large upward jumps and substantial radiative cooling in between the absorption of photons. As the result, the grain temperature T will be strongly fluctuating with large excursions above and below T_{ss} .

1.12 Molecular clouds

1.12.1 Molecular lines

The most common molecular lines are optically thick. To handle radiative transfer of optically thick lines, we use an escape probability β , such that we can replace A_{ul} by $A_{ul}\beta$.

1.12.2 Radiative trapping

In many astrophysical situations, there is sufficient gas such that the photon emitted by a decay transition $X_u \rightarrow X_l$ has a high probability of being absorbed by another X_l . Therefore the photon has a low probability of escaping the cloud. This effect is called radiative trapping and has two effects:

1. It reduced the emission in the $X_u \rightarrow X_l$ photons emerging from the region
2. It acts to increase the level of excitation of species X relative to what would be there if photons could escape freely.

1.12.3 Effect of high optical depth and critical density

For a high optical depth, the escape probability decreases, as $\beta = \frac{1}{1+0.5\tau_0}$.

1.12.4 CO as an estimator for the H_2 mass

The conversion factor does not depend on the CO abundance, but does depend on T and n . The conversion factor is despite of these dependencies, remarkably constant throughout the Galactic disk. The conversion factor is not valid for galactic nuclei of metal poor systems.

Optically thin lines One of the ways of using CO to estimate H_2 mass is as follows. ^{13}CO emission is usually optically thin. ^{12}CO emission is usually optically thick. If we write down the radiative transfer equation for ^{13}CO and ^{12}CO , we have

$$I_\nu = (1 - e^{-\tau_\nu} B_\nu(T))$$

$$I_\nu = B_\nu(T)$$

Where we used $(1 - e^{-\tau_\nu} \approx 1$ for $\tau \gg 1$. From the second equation, we can immediately deduce the temperature T . If we assume the temperature of the ^{13}CO and ^{12}CO are the same (tricky!), we can derive the ^{13}CO column density since the optical density is given by

$$\tau = \frac{h\nu}{4\pi} (N_0 B_{01} - N_1 B_{10}) \phi(\nu)$$

And we measure the line profile $\phi(\nu)$. If we assume ratios for ^{13}CO to ^{12}CO and ^{12}CO to H_2 , we can find the true H_2 column density.

Optically thick lines are nice and bright and therefore easier to observe in distant galaxies etc. We can however only see the surface of a molecular cloud or galaxy. Standard approach is to define an X factor, scaling between the observed frequency-integrated CO intensity along a given line of sight and the column density of gas along that line of sight. The reason for this to work is that a spectral line contains much more information than continuum

emission. Consider optically thick line emission from a cloud of mass M and radius R at temperature T . The mean column density is now

$$N = \frac{M}{\mu m_H \pi R^2}$$

Where $\mu = 2.3$ is the mass per H_2 molecule in units of m_H . The total integrated intensity we expect to see from this line is

$$\int I_\nu d\nu = \int (1 - e^{-\tau_\nu}) B_\nu(T) d\nu$$

Suppose that this cloud is in virial balance between kinetic energy and gravity, ie $\mathcal{T} = \mathcal{W}/2$ so that $\dot{I} = 0$. The gravitational self energy is $\mathcal{W} = aGM^2/2$ where a is a constant of order unity that depends on the cloud's geometry and internal mass distribution. For a uniform sphere we have that $a = \frac{3}{5}$. The kinetic energy is $\mathcal{T} = \frac{3}{2}M\sigma_{1D}^2$ where σ_{1D} is the one dimensional velocity dispersion, including both thermal and non thermal components. We define the observed virial ratio as

$$a_{vir} = \frac{5\sigma_{1D}^2 R}{GM}$$

And hence

$$\sigma_{1D} = \sqrt{\frac{a_{vir}}{5} \frac{GM}{R}}$$

Which is relevant since

$$\tau_\nu = \tau_{\nu,0} \exp \left[-\frac{(v - v_0)^2}{2(v_0 \sigma_{1D}/c)^2} \right]$$

If we integrate over all velocities of emitting molecules we get

$$I_{CO} = \int T_{B,\nu} d\nu = 2T_B \Delta\nu = \sqrt{8 \ln \tau_{\nu_0}} \sigma_{1D} T$$

Thus the velocity integrated brightness temperature is simply proportional to σ_{1D} . We herefore have

$$\begin{aligned} X \text{cm}^{-2} (\text{K km s}^{-1})^{-1} &= \frac{M/(\mu \pi R^2)}{I_{CO}} \\ &= 10^5 \frac{(\mu m_H \tau_{\nu_0})^{-1/2}}{T} \sqrt{\frac{5n}{6\pi a_{vir} G}} \end{aligned}$$

This is a simplified version of a more general technique, called the large velocity gradient approximation. The basic idea is the same: the total luminosity that escapes will be determined not directly by the amount of gas, but instead by the range in velocity of frequency that the cloud occupies, multiplied by the gas temperature.

1.12.5 Virial equilibrium

Molecular clouds are mostly in virial equilibrium. They are self gravitating objects. Their mass is dominated by unobservable H_2 but we use CO as a mass probe, even when it is optically thick.

1.12.6 Larson's relations

Larson's relations show that

1. The turbulence of a cloud is proportional to the cloud size.
2. The velocity dispersion is proportional to the cloud mass
3. The cloud size is inversely proportional to the density of a cloud

1.13 Shocks, supernova remnants and the 3-phase ISM

1.13.1 What is a shock?

A shock wave is a pressure-driven compressive disturbance propagating faster than the signal speed: a hydrodynamic surprise. Shock waves produce an irreversible change in the state of the gas (or fluid).

1.13.2 Physics of shocks

A shock has mass conservation, momentum conservation, energy conservation and magnetic flux conservation.

1.13.3 C type and J type shocks

If the cooling time is long compared to the time for a shock to pass (fast shock, low density), cooling can be ignored and we have an "adiabatic shock". There is no heat removed during the shock.

If the post-shock gas radiates lines, then it cools down and we have a radiative shock.

	J-type (jump)	C-type (continuous)
Velocity	$v_s > 50 \text{ km s}^{-1}$	$v_s < 50 \text{ km s}^{-1}$
How	Shock abrupt	Gas variables change continuously
Constituents	Molecules are mostly destroyed but reform in the cooling post-shock gas	The gas is heated but molecules are mostly not destroyed
Neutrals and ions	are tied into a single fluid	ions ahead of neutrals, drag modifies neutral flow
Radiation	Mostly in UV	Mostly in IR
Importance		Can be important in gas heating mechanisms

1.13.4 Sketch of J and C type shocks

1.13.5 Supernova shocks

Supernova shocks have a number of phases:

1. Early phase: Here the swept mass is lower than the ejected mass. There is free expansion and we have $R_S = v_s t$.
2. Sedov-Taylor phase ($M_{swept} > M_{eject}$ and $t < t_{cool}$). We have an adiabatic shock and lower expansion.
3. Snowplow phase ($t > t_{cool}$). Radiative shock and even slower expansion
4. Merging phase: v_s drops below velocity dispersion of ambient ISM.

1.13.6 Structure of SN remnant

The remnant of a supernova is as follows:

1. We have a hot interior with shocked ISM. The shocked ISM did not cool radiatively.
2. More outward, we still have shocked ISM, but here we do have radiative cooling and thus a cooler shell.
3. The remnant ends with the shock front
4. Outside the shockfront we have unshocked ISM

1.13.7 3-phase ISM model

In the 2-phase ISM model described so far, we only account for the WNM and CNM. We however still have the HIM (hot ionized medium). With the MW supernova rate, lifetimes and sizes, the neutral medium will be destroyed on timescales less than one million years. Vertical height of the CNM/WNM can only be explained if the medium is turbulent. Something must be stirring up the ISM continuously.

Overlapping SNRs create a tunnel system of hot ionized gas threading the HI clouds. SNR evolves in isolation until it intersects a tunnel and connects to the HIM. Then pressure drops suddenly as SNR vents to tunnel system and contributes to pressure of HIM.

Important features of the 3-phase model are:

1. Predicts pressure of the ISM correctly
2. Observed soft X-ray background in rough agreement with expectations from cooling of SNR gas.
3. Predicted cloud velocity dispersion agrees with observations
4. Does however not predict enough WNM
5. Requires proppity is larger than observed

1.14 Extra topics

1.14.1 PDRs and XDRs

X-rays penetrate much larger column densities than UV photons. Gas heating efficiency in XDRs is 10%-50%, compared to $< 1\%$ in PDRs. Dust heating is much more efficient in PDRs than XDRs. Using XDR, one can have stronger CO emission, especially in the higher J levels.

XDR mostly for AGN which radiate in x-ray. PDR mostly in star formation, where most of the photons are in the UV regime.

2 Formulas and tips

Radiative transfer equation in case of background and intermediate source with known τ_0

$$T_B = T_{background} e^{-\tau_0} + T_{source}(1 - e^{-\tau_0})$$

Radiative transfer equation in case of background and intermediate source with known τ_0 in intensity units (for RL regime)

$$I_B = \frac{2k}{\lambda^2} [T_{background} e^{-\tau_0} + T_{source}(1 - e^{-\tau_0})]$$

Atomic hydrogen (H1) is found at range of temperatures, but distribution is bimodal. E.g. warm neutral medium with $T_w \sim 5000 K$ and cold neutral medium with $T_c \sim 70 K$. Line center optical depth (with C a constant)

$$\tau_o = \frac{CN}{T_S \sigma_v}$$

If we are looking at two layers (T_W, N_W and T_C, N_C) but assume it is one layer for which we known $\tau = \tau_c + \tau_w$ and $N = N_W + N_C$, we can calculate the effective measured temperature

$$\frac{C}{\sigma_v} \frac{N}{T_{eff}} = \frac{C}{\sigma_v} \left[\frac{N_W}{T_W} + \frac{N_C}{T_C} \right]$$

$$T_{eff} = \frac{N_C + N_W}{\frac{N_C}{T_C} + \frac{N_W}{T_W}}$$

Maser emission can occur when the process of populating a certain energy level is easier than that of other, lower levels. To have a maser in the $i \rightarrow j$ transition we need that

$$\frac{n_i}{n_j} > \frac{g_i}{g_j}$$

In radio regime, all small differences between hydrogen and helium cancel out when considering ratios. This is because at these high quantum levels, the nucleus is effectively just a point source with charge +1, because the electron is so far away from the nucleus. When observing both $H\alpha$ and $H\beta$ emission, we can probe the intrinsic flux.

$$\frac{S(H\alpha)}{S(H\beta)} = \frac{S_0(H\alpha)}{S_0(H\beta)} e^{-\tau_{H\beta} - \tau_{H\alpha}}$$

Now using eg $\tau_{H\beta} = 1.6\tau_{H\alpha}$, we can calculate $\tau_{H\alpha}$, since the intrinsic ratio is known from Case B recombination.

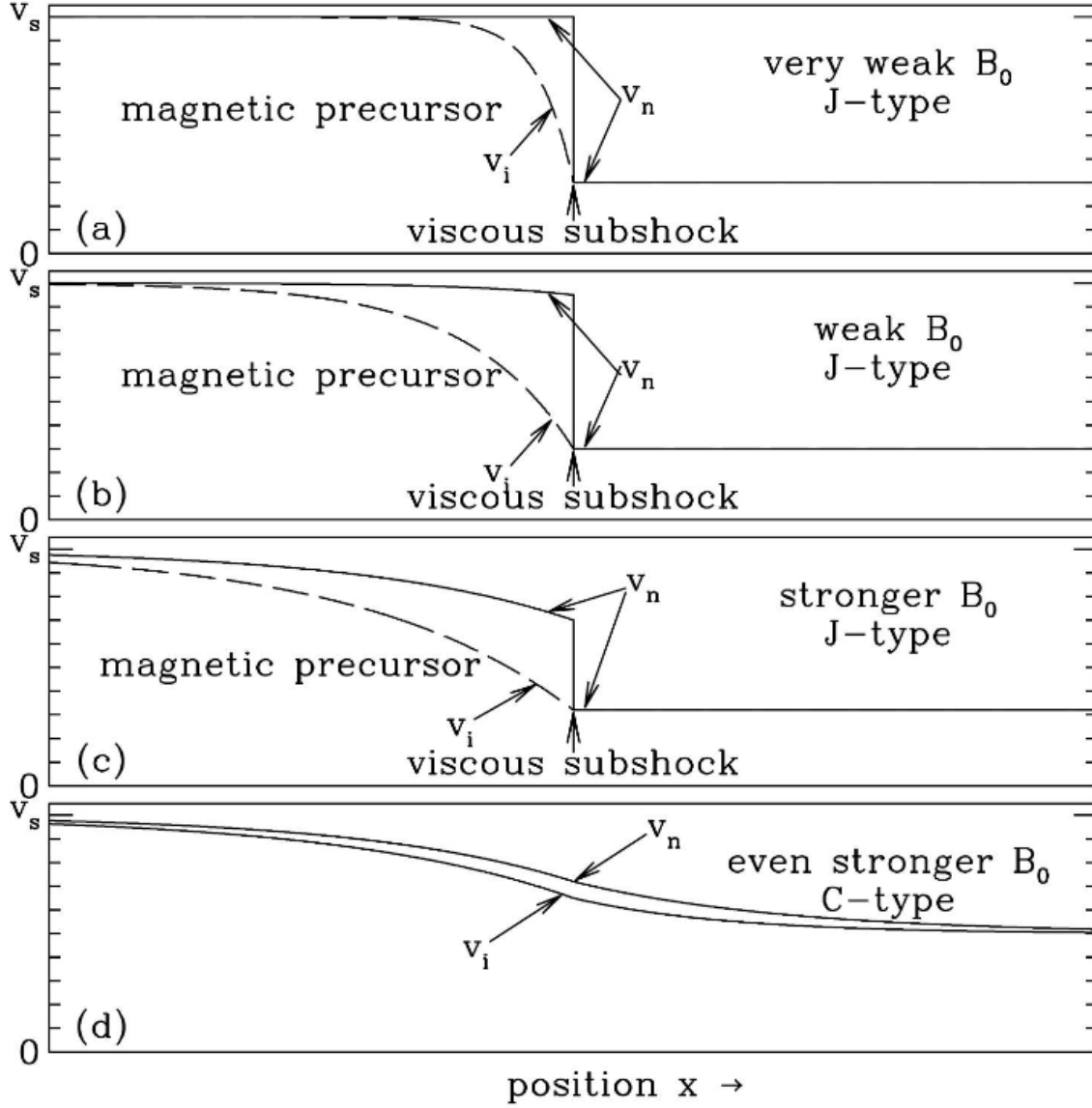


Figure 1: Schematic representation of J and C type shocks. Note that the J type shocks have a jump, which is diminished with increasing B_0 . C type shocks always have a continuous transition.

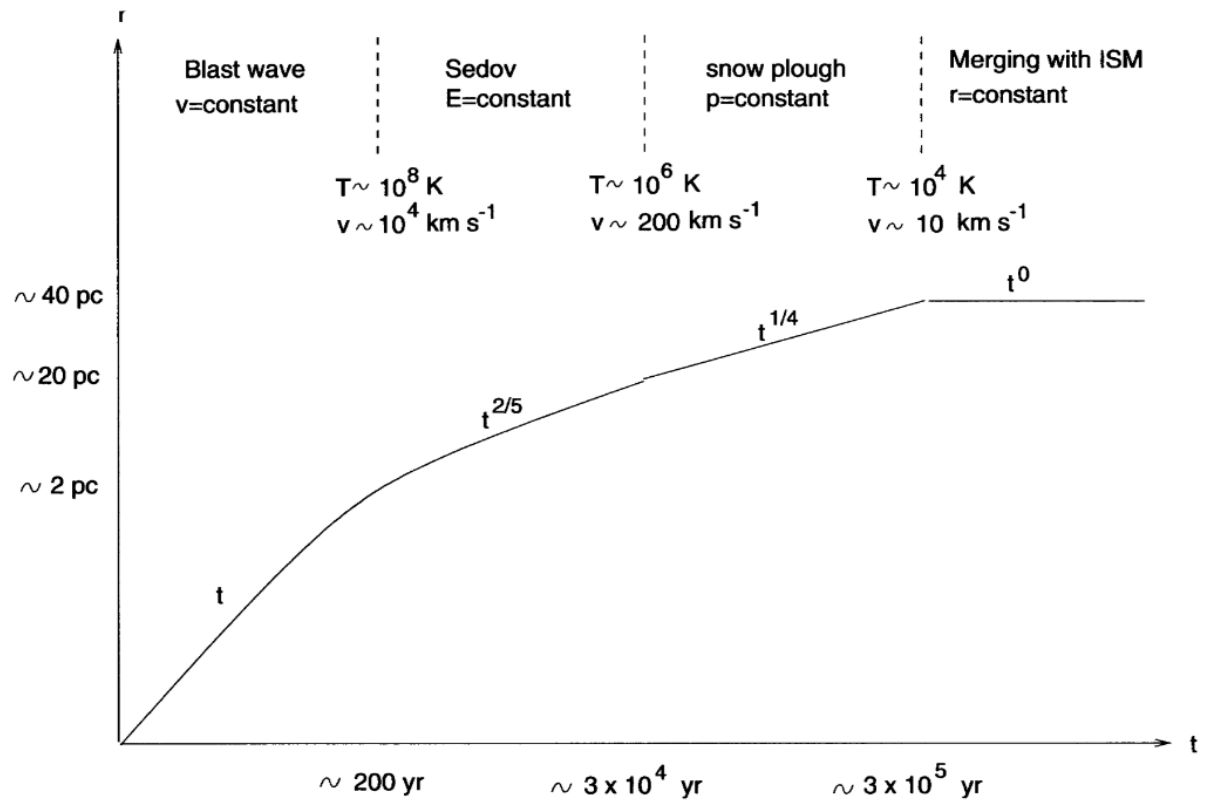


Figure 2: Schematical representation of a supernova shock with the different stages in it.